Scientific Contributions Oil & Gas, Vol. 49. No. 2, June: 393 - 408

SCIENTIFIC CONTRIBUTIONS OIL AND GAS

Testing Center for Oil and Gas
LEMIGAS

Journal Homepage:http://journal.lemigas.esdm.go.id
ISSN: 2089-3361, e-ISSN: 2541-0520

Multi-Objective Optimization of Risk-Based Inspection Planning for Oil and Gas Piping Systems Using NSGA-II Algorithm

Tri Wahono[1,2], Endah R.M. Putri[3], Imam Mukhlash[3], and Agung Purniawan[4]

[1]Department of Interdisciplinary School Management and Technology, Institut Teknologi Sepuluh Nopember
ITS Main Road, Keputih, Sukolilo District, Surabaya, East Java 60111, Indonesia

[2]Asset Integrity & Reliability, PT Pertamina Hulu Rokan,
Prof. DR. Satrio Street No. 30, RT. 17/RW. 4, Karet Kuningan, Setiabudi Subdistrict, South Jakarta City, 12940

[3]Department of Mathematics, Institut Teknologi Sepuluh Nopember
ITS Main Road, Keputih, Sukolilo District, Surabaya, East Java 60111, Indonesia

[4]Department of Materials and Metallurgical Engineering, Institut Teknologi Sepuluh Nopember
ITS Main Road, Keputih, Sukolilo District, Surabaya, East Java 60111, Indonesia

Corresponding author: Endah R.M. Putri (endahrmp@matematika.its.ac.id)

Manuscript received: February 27th, 2026; Revised: April 01st, 2026
Approved: May 04th, 2026; Available online: June 15th, 2026; Published: June 15th, 2026.

ABSTRACT - The systematic examination of piping is essential in the successful implementation of risk-based inspection (RBI). The ineffective execution of this activity increases the risk of equipment failure and unnecessary costs. Therefore, this study aims to address the challenge of optimizing inspection planning for oil and gas piping systems in budget and operational constraints. The most effective inspection methods were selected to determine the optimal inspection interval. A multi-objective optimization model based on non-dominated sorting genetic algorithm-II was also applied to simultaneously minimize probability of failure as well as optimize total inspection costs. The adopted methodology, which is dissimilar to traditional methods, eliminated reliance on predefined risk thresholds and explicit failure-consequence evaluations by directly incorporating inspection costs. Additionally, the best-performing model achieved an efficient solution by reducing the total probability of failure from 1.631 10^{-1} to 0.8975 10^{-1}. The application model further provided a robust decision-support tool for efficient inspection planning, increased inspection effectiveness, and reduced risk of failure (RoF). The developments formed the basis for effective decision-making to support the implementation of asset integrity management through efficient inspection planning.

Keywords : inspection planning, multi-objective optimization, oil and gas, piping, risk-based inspection.

How to cite this article:

Tri Wahono, Endah R.M. Putri, Imam Mukhlash, and Agung Purniawan, 2026, Multi-Objective Optimization of Risk-Based Inspection Planning for Oil and Gas Piping Systems Using NSGA-II Algorithm, Scientific Contributions Oil and Gas, 49 (2) pp. 393 - 408. DOI org/10.29017/scog.v49i2.2084.

INTRODUCTION

The equipment supporting oil and gas operations is presumed to face challenges posed by complex related procedures and aging facilities (Asyik et al., 2026). Inspection is the main tool for verifying that all equipment in production facilities is in optimal condition for operational functionality. It also ensures the prevention of damages in advance. However, inspecting all equipment equally is inefficient, considering the extremely large and complex number of operation facilities (Rachman & Ratnayake 2019). The asset integrity management system also plays an important role in preventing failure. The process is actualized by reducing degradation, minimizing risk, and ensuring the safe operation of lifecycle assets (Wahono et al., 2025). Risk-based inspection (RBI) has become a central solution in the new global economy to reduce excessive financial losses, including impairment, for companies in oil and gas sector (Aditiyawarman et al., 2023).

Based on this perspective, RBI was conducted to develop an optimal plan for inspection implementation, alongside improving safety and integrity to maintain efficient operations and equipment (Campari et al., 2024). This also offered a common framework for evaluating equipment risk, as well as facilitated the identification of connections between breakdown mechanisms and related failure modes (Abubakirov et al., 2020). Meanwhile, a typical example of a lack of an inspection program for piping systems is Richmond refinery pipe rupture and fire case (Weber 2006). This led to the two main activities of RBI program, namely risk assessment and inspection planning (API RP 580 2023). Previous studies reported that inspection planning has several challenges, namely prioritizing the equipment to inspect, determining when to conduct inspection, and selecting the most appropriate method based on risk level.

Considering the widespread adoption of RBI in oil and gas sector, existing inspection planning methods often depended on deterministic or single-objective methods. These processes do not adequately account for trade-offs between safety and inspection costs. For example, Teurupun et al., (2024), proposed RBI methodology for pressure safety valves and stripper acid gas removal with a fixed inspection interval. Reliability-based FFS studies focused on predicting present risks and determining the remaining life, including the ability of the equipment to withstand internal pressures since the last inspection. Seo et al. (2015) reported that it was difficult to accurately predict inspection planning, alongside the level of risk encountered during the operating period. The determination of inspection intervals was also based on probability of failure and the potential undesirable effects of the transferred fluid (Sözen et al., 2022). With budget constraints, RBI not only reduces failures but also minimizes costs.

Several studies have advanced RBI planning in recent years. For example, Moura et al. (2015) proposed coupling RBI methodology with multi-objective genetic algorithm (MOGA). The study focused on oil and gas separator vessel that experienced both internal and external corrosion, leading to material thinning. The results showed that the methodology provided an effective tool for making efficient decisions concerning equipment mechanical integrity. In 2019, Abubakirov et al. (2020) introduced a method for determining optimal inspection intervals for underground oil pipelines. This study used a utility function to optimize the inspection interval by combining risk and annual related program cost. Y. Javid (2025) developed inspection optimization methods in the petrochemical industry to reduce overall risk exposure while optimizing expenditures. This included the integration of RBI principles with a novel two-objective mathematical model, which led to the formulation of a comprehensive framework for equipment inspection programs.

In line with the optimization method proposed by previous studies, the implementation across multiple industries and equipment categories remained inadequately investigated. Considering the identified gap, this study addressed the earlier mentioned challenges by developing a multi-objective optimization framework for planning oil and gas piping RBI. The proposed framework simultaneously optimized inspection intervals, safety performance, and costs to support more effective decision-making regarding planning. Additionally, the framework aimed to improve the efficiency and reliability of piping inspection programs. The entire procedure was actualized by integrating risk assessment with multi-objective optimization.

This study aims to show the application of a multi-objective optimization perspective to RBI planning. A case study dataset of piping systems were adopted for the upstream oil and gas sector. The benefits of the proposed method were evaluated by comparing it with the conventional method, namely manual inspection planning.

Based on this perspective, the remaining part of the study was organized as follows in the subsequent sections. The second section focused on the study methodology, which comprised RBI method per API RP 581 and multi-objective optimization using non-dominated sorting genetic algorithm-II (NSGA-II). This was followed by the third section, which provided the results and analysis. Finally, the fourth section centered on the concluding aspect of the study.

METHODOLOGY

The proposed method in Figure 1 aims to balance optimization objectives by minimizing the risk of piping system failure and inspection costs alongside satisfying expenditure and operational constraints. API RP 581, the common practice standard for RBI, stated that risk of failure (RoF) model integrates probability and consequences. Inspection costs are calculated based on three components, namely related method, personnel, and equipment downtime expenses. The purpose was supported by using a multi-objective optimization model which integrating NSGA-II (Deb et al., 2002; Javid 2021).

Risk-based inspection

Risk-based method prioritized equipment in line with risk of failure. The prioritization enabled an organization to focus inspection efforts on high-risk equipment. Previous studies reported that it prevented over-inspection of low-risk equipment

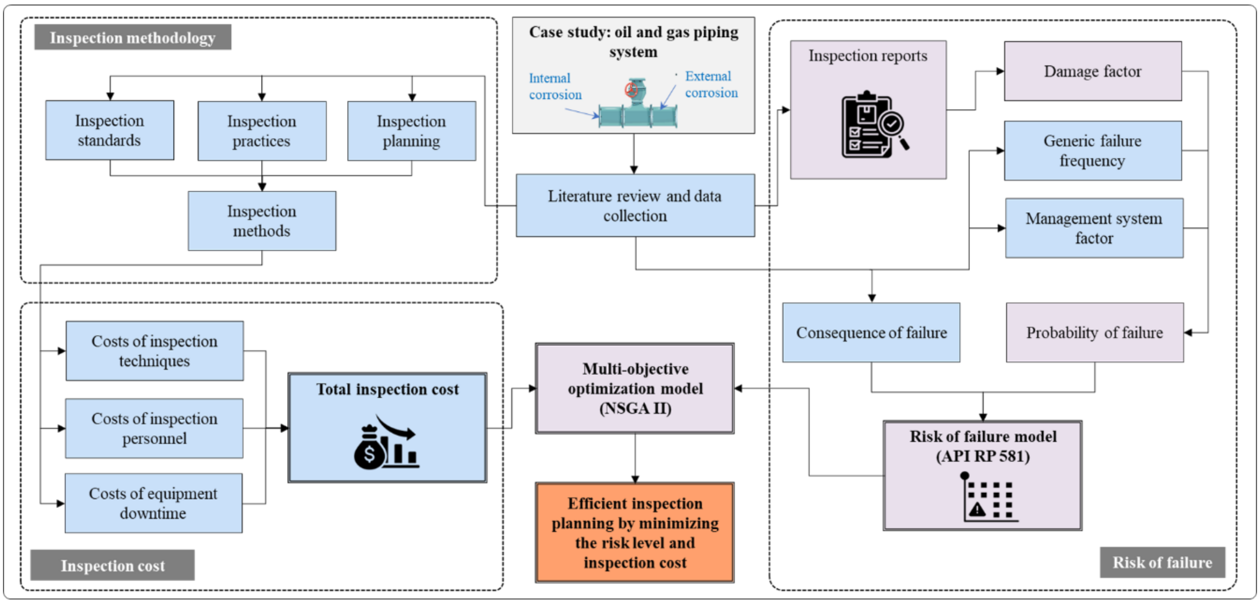

Figure 1. The proposed multi-objective optimization model framework for RBI planning.

(Rachman & Ratnayake 2019). Furthermore, the reference used in RBI determination is API RP 581 (API RP 581 2025). In RBI, risk of failure refers to the result of integrating probability of failure (PoF) with the consequences (CoF). This section provides a contextual analysis of the quantitative RBI methodology. The processes of estimating probability of failure *Pf(t)* and the financial consequences (FC) were outlined to determine the risk level *R(t)* over time (t).

The representative example of inspection planning is shown in Table 1, where six-time intervals alongside three distinct inspection methods were clarified. In addition, inspection method 1 was applied during the first and fourth periods. Methods 2 and 3 were implemented in the second to fifth, and third to sixth periods, respectively.

Probability of failure

The probability of failure is associated with a specific damage mechanism, denoted as *w* which is calculated using the following Equation 1

$$P^{h}_{f\_w}(t) = gff^{h} \cdot D^{h}_{f\_w}(t) \cdot F_{MS} \quad (1)$$

where t represents a specific time frame, and h denotes the size of the release hole. Additionally, four distinct values for h were considered 0.25", 1", 4", and 16", and these corresponded to small, medium, large, and rupture, respectively. In the generic failure frequency (gff^h) for a particular piece of equipment and hole size, h was derived from a representative failure database. The equation $gfftotal = \sum h\, gff^{h} \cdot$ $D^{w}_{f}(t)$ refers to the damage factor and the generic failure frequency corresponding to a specific mechanism of failure (w). The management system factor that reflects how the facility influences the mechanical integrity of the plant is F_{MS}. It is often assessed through a questionnaire that produces scores ranging from 0 to 1000. F_{MS} = $10^{(-0.02 \cdot pscore + 1)}$, where $pscore$ = $0.1 score$. Therefore, $P^{h}_{f\_w}(t)$ is calculated for failure mechanism w with different hole sizes h. The equation shows that the only aspect subject to change over time is $D^{w}_{f}(t)$, which functions as a time-dependent variable, while the factors gff^h and F_{MS} remain constant. This study focused on failure mechanism of piping systems due to corrosion, both internal (w_1) and external (w_2).

Calculation of the damage factor

$D^{w}_{f}(t)$ is the damage factor derived from data gathered during prior inspection. The outcomes showed that corrosion rates (r) have inherent uncertainties, which directly affected the calculations of $D^{w}_{f}(t)$ and $P^{h}_{f\_w}(t)$. Therefore, increasing the confidence level when determining corrosion rates depended on the effectiveness of inspection methods.

The metal loss parameter, A_{rt}, is the duration of the last inspection (age) and the corrosion rate, which is calculated as Equation 2

$$A^{w}_{rt}(t,i) = \left[\left(1 - \frac{t^{w}_{rd}(t,i) - r_i \cdot age}{t_{min} + C_{allow}}\right), 0.0\right] \quad (2)$$

where t_{rd} represents the thickness reading, t_{min} denotes the minimum required wall thickness, and C_{allow} depicts the corrosion allowance.

The damage factor, was determined by considering *Art*, alongside the quantity and effectiveness of prior inspection. Subsequently, it was adjusted using Equation 3, with F_{OM}, F_{IP}, F_{DL}, F_{WD}, F_{MA}, and F_{SM} as adjustment factors.

$$D_{f_w}(t,r_i) = \frac{D_{f_w}(t,r_i) \cdot F_{IP} \cdot F_{DL} \cdot F_{WD} \cdot F_{MA} \cdot F_{SM}}{F_{OM}} \quad (3)$$

Ineffective inspection methods led to a distinction, and the actual corrosion rate (r) became uncertain, potentially deviating from the calculated value. The effectiveness of an inspection method was measured as probability that its values

Table 1. Typical inspection plan

	Method 1						Method 2						Method 3					
Period	1	2	3	4	5	6	1	2	3	4	5	6	1	2	3	4	5	6
Inspection plan	0	1	0	0	1	0	1	0	1	1	0	0	1	0	0	0	0	1

accurately reflected piping actual corrosion condition. The more effective the inspection results, the higher the likelihood of matches between predicted and actual corrosion rates. This method effectively minimized the uncertainty related to the corrosion rate, as well as subsequent uncertainties in $D_f^w(t)$ and $P_{f\_w}^h(t)$. The damage factor $D_{fw}(t,ri)$ varied following the values of the diverse types, namely 1 ($r_1 = r$), 2 ($r_2 = 2r$), and 3 ($r_3 = 4r$). Equation 5 was used to calculate the value of considering the variation of estimated hole sizes (h).

$$P_{f\_w}^h(t) = \sum_{i=1}^{I} P_{f\_w}^h(t, r_i) \cdot \pi_t(r_i), for\ t = 0, \quad (4)$$

$$P_{f\_w}^h(t) = \sum_{i=1}^{I} P_{f\_w}^h(t, r_i) \cdot \pi_t(r_i|r), otherwise, \quad (5)$$

where t > 0, Equation 4 was used to update the confidence in failure state rate. $P_{f\_w}^h(t)$ changes over time were reflected in the effectiveness of the inspection during each period. Probability of failure associated with failure mechanism w is equivalent to the total sum. This corresponded with the various hole sizes and was calculated using Equation 6.

$$P_{f-w}^h(t) = \sum_{h=1}^{I} P_{f-w}^h(t) \quad (6)$$

The total probability of failure at period t was computed using Equation 7. The calculation was repeated twice, for each failure mechanism, namely internal and external corrosion.

$$P(t) = \sum_{w=1}^{w} P_{f-w}^h(t) - \prod_{w=1}^{w} P_{f-w}^h(t) \quad (7)$$

Table 2 shows the classification of effectiveness inspection into five distinct levels, with A and E representing the highest and lowest degree of effectiveness, respectively. Therefore, greater accuracy and effectiveness in terms of detecting the corrosion mechanism "w" were associated with more expensive inspection methods. These increased probability of detection as well as improved the accuracy of predicting the corrosion rate.

Consequence of failure

Financial terms (FC) represent the consequences of failure. This procedure outlines the steps for analyzing the consequences of equipment operating at constant pressure. According to API RP 581, the consequence of

Table 2. Inspection effectiveness levels (API RP 581 2025).

Inspection effectiveness description	The inspection effectiveness levels	Description
Highly Effective	A	Inspection methods are expected to accurately show the extent of damage in every situation, with a confidence level of 80% to 100%.
Usually Effective	B	The inspection methods should accurately determine the actual damage condition most of the time, with a confidence level ranging from 60% to 80%.
Fairly Effective	C	The inspection methods should accurately determine the actual damage condition approximately half of the time, with a confidence level between 40% and 60%.
Poorly Effective	D	The inspection methods should offer limited information for accurately determining the actual damage condition, with a confidence level of 20% to 40%.
Ineffective	E	The inspection methods should provide minimal to no information for accurately determining the actual damage condition, as well as considered ineffective for detecting the specific damage mechanism, with less than 20% confidence.

failure is kept constant over time. It is calculated using Equation 8 by summing up overall costs.

$$FC = FC_{cmd} + FC_{affa} + FC_{prod} + FC_{inj} + FC_{environ} \quad (8)$$

Level 1 consequence analysis mainly focuses on assessing the impact of releasing hazardous liquids by evaluating hole size (h) and overall costs. API RP 581 classified these costs by considering the cost for performing repair and replacement (FC_{cmd}) for damaged piping systems. In addition, this cost is calculated using Equation 9

$$FC_{cmd} = \left(\frac{\sum_{h=1}^{4} gff^{h} \cdot holecost^{h}}{gff_{total}}\right) \cdot \text{matcost} \quad (9)$$

where *holecost*^{h} is the cost of equipment repair related to steel price. Other materials used *matcost* as a cost factor to update *FCcmd.* In the event of a fire explosion, the cost of failure to adjacent piping systems in the affected areas (FC_{affa}) was also computed using Equation 10

$$FC_{affa} = CA_{cmd} \cdot equipcost \quad (10)$$

where CA_{cmd} denotes the total consequence area (m^2), and the cost of replacing the process unit per square meter ($/$m^2$) represents the *equipcost*. When assessing the costs of repairing or replacing damaged piping systems, it is crucial to factor in both operational downtime and resulting production losses. The costs associated with the calculations covered damaged piping systems and all equipment affected in the area, starting from the time of failure for each piece of equipment. The calculation costs are stated using Equation 11

$$FC_{prod} = Outage_{cmd} \cdot Outage_{affa} \cdot \text{prodcost} \quad (11)$$

where $Outage_{cmd} = (\sum_h gff^h \cdot Outage^h / gff_{total}) \cdot Outage_{mult}$ is the weighted duration to restore piping systems during the investigation (measured in days). $Outage^h$ refers to the number of days required to repair damages associated with the release hole size h. The increase factor of the equipment hole size was denoted as $Outage_{mult}$. The duration (days) required to repair equipment in the affected area is $Outage_{affa}$. Additionally, $prodcost$ represented the daily production loss cost incurred during therepair process ($/day). Equation 12 was used to calculate the cost associated with hidden personnel and community impacts.

$$FC_{inj} = CA_{inj} \cdot \text{popdense} \cdot \text{injcost} \quad (12)$$

where CA_{inj} represents the people impact area (m^2), *popdens* is the people or workforce density per square meter (people/m^2), and *injcost* depicts the cost related to serious injuries or people fatalities ($). The cost of environmental cleanup is calculated using Equation 13

$$FC_{environ} = \left(\frac{\sum_{h=1}^{4} gff^{h} \cdot vol_{env}^{h}}{gff_{total}}\right) \cdot \text{envcost} \quad (13)$$

where *envcost* refers to the cost of environmental cleanup and vol_{env}^h is the leak rate during cleanup for each of the four distinct hole sizes.

The purpose of this study is to develop an efficient inspection planning framework. RBI method is prominent for its multi-objective nature and does not inherently necessitate the calculation of FC. According to API RP 581, FC remains constant over time, and probability of failure is updated only by recalculation of failure factor at interval t. This feature of RBI method greatly reduced the computational effort required to formulate an inspection plan in a multi-objective framework.

Problem statement and formulation

Problem of multi-objective optimization included selecting efficient inspection programs x that balanced between $P_f(x)$ and $C(x)$, was formally described as follows (Javid 2025)

$$MinP_f(x) = \sum_{t=1}^{m} p_f(t) \quad (14)$$

Equation 14 was designed to minimize the overall risk level, specifically by reducing the total probability of failure. Additionally, the essence was to establish the most efficient inspection plans (Javid 2025).

$$MinC(x) = \sum_{j=1}^{n}\left(C_j \sum_{t=1}^{m} X_{j,t}\right) + \sum_{j=1}^{n} C_{p,j} \sum_{t=1}^{m} X_{j,t} + \sum_{j\epsilon j'} C_{d,j} \sum_{t=1}^{m} X_{j,t} \quad (15)$$

In this equation, the total probability of failure during period t is denoted by , where t ∈ T = {1, 2,…, m} signifies the various time frames. The objective was to minimize the overall RBI cost, as determined by Equation 15. The total cost consisted of inspection method, personnel, and downtime costs. In this context, C_j depicts the cost associated with conducting an inspection using method type j, $C_{p,j}$ refers to the personnel cost per inspection of type j. $X_{j,t}$ is assigned a value of 1 if inspection method j is performed within time (t), otherwise it is 0. $C_{d,j}$ represents the cost of operational downtime per inspection of type j. Furthermore, j ∈ J = {1, 2,…, n refers to different types of inspection methods, and j ∈ J′ = {1, 2,…, n} pertains to the methods of inspection that demand a shutdown. Multi-objective model established RBI program, which depended on the following assumptions:

- Any inspection method is permissible.
- Various inspection methodologies can be adopted at any stage.
- Minimizing the total probability of failure is the main objective function.
- Minimizing overall inspection costs is the subsequent objective function.
- The inspection duration must not exceed the maximum permitted time.
- A single effectiveness inspection technique can be used for any corrosion rate.
- The corrosion rate associated with the degradation mechanism must remain below the permissible corrosion rate.

Multi-objective optimization model

In the field of multi-objective optimization, a solution that simultaneously supports all objectives, considering the often exhibited conflicting characteristics tends to be rare. The solution obtained represents a set of efficient, or non-dominated, outcomes that reflect trade-offs among the objectives. It is considered non-dominated if the improvement of one or more objectives deteriorated an equivalent number of other objectives, as formally stated in Equation 16 (Javid 2025).

$$x^1 \succ x^2 \Leftrightarrow f_i(x^1) \le f_i(x^2), \forall i \quad and \; f_i(x^1) < f_i(x^2), \text{for some } i, \quad (16)$$

where dominatesin a minimization problem. However, when these conditions are not fully satisfied, both solutions tend to be efficient, with each dominating the other in certain objectives. These collectively formed Pareto frontier, where all solutions were considered equally valid. MOGA based on non-dominated sorting genetic algorithm II (NSGA-II) was proposed. The algorithm enabled genetic operators to generate only feasible inspection intervals, which led to the reduction of the search space, thereby avoiding the exploration of infeasible regions. It also minimized unnecessary fitness evaluations, as well as eliminated the need for penalty functions.

Initial population generation

The process of initial population generation was described using a sample case. The representation of the initial solution shows a sequence of binary numbers corresponding to the decision variables. The maximum intervals for a scenario across 6 periods using 3 inspection methods, are $t_{1,\ max} = 3$; $t_{2,\ max} = 5$; and $t_{3,\ max} = 7$. Therefore, if an equipment is inspected using method 1 during the second period, the next inspection using the same method must be conducted within < 3 periods.

Crossover operator

Segments of chromosomes from the current generation were swapped to generate new offspring during the crossover process. In addition, this study used two-point and uniform crossover method. The two-point crossover, with a given chromosome vector (e.g., 1 × 6 for one inspection method over six periods), led to the selection of 2 parents and random points along the chromosome. The genes between these points were then swapped to generate offspring. All chromosome positions were considered in uniform crossover, with a randomly generated binary mask used to determine which parent contributed a specific gene to the first child. Meanwhile, the second child was determined by reversing the mask assignment. Considering that uniform crossover increases population diversity, it does not preserve the memory of each chromosome as effectively as a two-point crossover. Figure 2 shows the case of a single-point intersection function applied to the variable X chromosome. The two-point crossover method entailed the selection of two random points, with the gene values exchanged between the parent chromosomes, rather than the preference for a single random point. Figure 3 shows the application of a two-point crossover on a variable X chromosome.

Mutation operator

The mutation operator introduced random chromosomal changes, including genes absent from the original population. This study initially applied a comprehensive mutation, namely a random number between 0 and 1 was generated for each gene. If the random number is less than 0.1, then the gene is inverted (1 becomes 0, and 0 becomes 1).

The mutation enhanced diversity, as shown in Figure 4. Additional innovative mutations were further applied to improve the efficiency of the metaheuristic algorithm and quicken convergence toward Pareto-optimal solutions. This was shown using a sample chromosome of dimensions 6 × 3 (six time periods and three inspection methods).

The selection of a particular solution from Pareto set for practical application generally depended on the strategic preferences and priorities of the decision-maker or stakeholders (Omar & Moselhi, 2026. The process was supported by

Period	*1*	*2*	*3*	*4*	*5*	*6*
Parent 1	*0*	*0*	*1*	*0*	*1*	*1*
Parent 2	*0*	*1*	*1*	*0*	*1*	*0*

Period	*1*	*2*	*3*	*4*	*5*	*6*
Offspring 1	*0*	*0*	*1*	*0*	*1*	*0*
Offspring 2	*0*	*1*	*1*	*0*	*1*	*1*

Figure 2. An representation of a single-point intersection function on a variable X chromosome.

Period	*1*	*2*	*3*	*4*	*5*	*6*
Parent 1	*0*	*0*	*1*	*0*	*1*	*1*
Parent 2	*0*	*1*	*0*	*1*	*0*	*0*

Period	*1*	*2*	*3*	*4*	*5*	*6*
Offspring 1	*0*	*0*	*0*	*1*	*0*	*0*
Offspring 2	*0*	*1*	*1*	*0*	*1*	*0*

Figure 3. An representation of a two-point crossover operation on a variable X chromosome.

adopting various strategies, either individually or by combining it, such as:

- Simple preference-based methods: Decision-makers determined weights or priorities to define an objective. This was actualized by referring to criteria including acceptable risk and budget constraints, as well as selecting Pareto solution that best reflected the preferences.
- Multi-criterion decision-making methods: AHP, TOPSIS, and weighted sum ranked Pareto solutions by combining several objectives into a single weighted score to identify the best option.
- Clustering-based methods: Pareto solutions were grouped into categories, enabling stakeholders to select a cluster and a representative solution that best fits respective priorities.
- Trade-off-based (compromise) solution methods: This included knee-point and utopia-point methods, which assisted in the selection of balanced Pareto solutions. The process was carried out by identifying trade-offs or selecting the option closest to an ideal (elbow) method that identified Pareto solution. Additionally, a slight improvement in an objective led to a large change in the other (Huang, 2020; Tang et al., 2023; Zhang et al., 2021. Another method is the selection of the closest solution to the ideal scenario (minimum total cost and PoF), also known as utopia (ideal) point method (Niu & Li, 2025; Omar & Moselhi, 2026; Szparaga et al., 2019. In this context, utopia method was used to determine efficient solutions.

Case study and model implementation

The proposed method was applied using real data from oil and gas piping systems. This equipment is critical for processing hydrocarbons while ensuring operational continuity and managing fluctuating demand. Piping systems were selected as the main case study because of the extensive network, high exposure to degradation mechanisms, and significant influence on overall plant reliability. When compared to other static equipment, the pipes showed a higher failure rate and were more prone to leaks and ruptures, leading to unplanned shutdowns, safety hazards, and substantial economic losses. A higher failure rate was also observed, because the pipes were prone to leaks and ruptures. This led to unplanned shutdowns, safety hazards, and substantial economic losses. Furthermore, due to the scale and high failure frequency, piping systems posed complex inspection challenges, offering an ideal case study for RBI optimization. Piping information data is shown in Table 3. The proposed NSGA-II method was further applied to generate non-dominated inspection programs.

Inspection was planned for a 20-year time horizon, using 3 common methods, namely ultrasonic thickness measurement (UTM), guided wave testing (GWT), and hydrostatic testing (HT). These methods varied in respective effectiveness at identifying internal and external flaws.

Tables 4 and 5 show supplementary data gathered from the facilities, such as initial and minimum thicknesses, corrosion rates for internal and external surfaces, alongside inspection

Period	*1*	*2*	*3*	*4*	*5*	*6*
Parent 1	*0*	*0*	*1*	*0*	*1*	*1*

Period	*1*	*2*	*3*	*4*	*5*	*6*
Offspring 1	*0*	*1*	*0*	*1*	*1*	*1*

Figure 4. An representation of a mutation function on a variable X chromosome.

Table 3. Piping information data.

Parameter	Data
Diameter (inch)	24
Nominal thickness (mm)	6.35
Segment length (m)	500
Service life (years)	26
Operating pressure (psig)	260
Operating temperature (°F)	200
Service fluid	Crude oil
Construction material	CS API 5L B PSL 2
Piping condition	Aboveground

Table 4. The parameter of the case study.

Method	C_j	$C_{p,j}$	$C_{d,j}$	$t_{j,max}$	Inspection effectiveness in detecting internal corrosion	Inspection effectiveness in detecting external corrosion
j = 1 (UTM)	1,000	300	0	3	C	C
j = 2 (GWT)	5,000	500	0	5	B	B
j = 3 (HT)	10,000	1,000	10,000	15	A	A

Table 5. Supporting parameters to solve the case study.

Parameters	Value
r	0.1 mmpy
t_{rd}	5 mm
t_{min}	4.17 mm
$F_{MA} = F_{OM} = F_{IP}=F_{SM}=F_{MS} = F_{DL} = F_{WD}$	1
gff	0.0000306
C_{allow}	1 mm

frequency. This also included the effectiveness of different inspection methods in detecting defects, associated costs, reducing factors, as well as personnel and equipment downtime. Further details required to complete the model, including the general failure factor and metal loss rate, were also provided in accordance with API RP 581.

The period, quantity of inspection methods, frequency, types of damages encountered, sizes of holes, and, most significantly, aggregate of prior inspection alongside respective effectiveness, are shown in Table 6 All sourced data were collected from oil and gas piping systems operating at a gathering station of an upstream processing facility. The critical factors in NSGA-II that influence problem-solving mechanism should be properly configured. Furthermore, the main variables that influenced problem-solving process included:

- Maximum iterations: The proper setting of the maximum iteration parameter is essential for reducing the time required to solve the problem as well as obtaining nearly optimal solutions.

- Initial population: The accurate determination of its size is crucial in terms of achieving a diverse, representative set of solutions, ensuring that all potential solutions are addressed.
- Mutation and crossover rate: These parameters influenced the algorithm balance between exploration and exploitation. If the values are not set correctly, the algorithm may lose the historical memory.

The parameter used to address the case study problem is shown in Table 7. Furthermore, the optimal parameter was developed through a combination of experiences, including trial-and-error.

RESULT AND DISCUSSION

Based on this context, tables 8 and 9 focused on comparing the initial and effective solutions. Table 8 specifically shows that the inspection process carried out with the UTM method must be conducted in the period 3-6-9-12-15-18. GWT and HT methods must also be conducted in the periods 5-10-15-20, and 15, respectively. The initial inspection program was determined based on the maximum time required for each method. Meanwhile, the results of the optimal inspection planning from NSGA-II simulation are shown in Table 9. This implied that the inspection process carried out with UTM, GWT, and HT must be

Table 6. The size of the case study.

Variables	Value
Inspection period	20
Inspection method	3
Hole size	4
Damage mechanism	2
Total of prior inspection and effectiveness of internal corrosion (w_1)	1D
Total of prior inspection and effectiveness of external corrosion (w_2)	1D

Table 7. Parameters of NSGA-II algorithm.

Parameter	Optimum value
Initial population *Npop*	250
Maximum iteration *Maxit*	100
Mutation rate Pm	0.08
Crossover rate *Pc*	0.9

Table 8. Inspection methods over the time period used in the initial plan.

Period	1	2	3	4	5	6	7	8	9	10	11	12	13	14	15	16	17	18	19	20
j = 1 (UTM)	0	0	1	0	0	1	0	0	1	0	0	1	0	0	1	0	0	1	0	0
j = 2 (GWT)	0	0	0	0	1	0	0	0	0	1	0	0	0	0	1	0	0	0	0	1
j = 3 (HT)	0	0	0	0	0	0	0	0	0	0	0	0	0	0	1	0	0	0	0	0

Table 9. Inspection methods over time result in an efficient plan generated using NSGA-II.

Period	1	2	3	4	5	6	7	8	9	10	11	12	13	14	15	16	17	18	19	20
j = 1 (UTM)	0	0	1	0	0	1	0	0	1	0	0	1	0	1	0	0	1	0	0	0
j = 2 (GWT)	0	0	0	1	0	0	0	1	0	0	0	1	0	0	1	0	0	0	0	0
j = 3 (HT)	0	0	0	0	1	0	0	0	0	0	0	0	0	0	0	0	0	0	0	0

conducted in the periods 2-5-8-11-14-17, 2-7-11-16, and 7, respectively. The results met the established limitation rule because the inspection interval for each method remained in the maximum inspection interval.

Pareto-optimal solutions obtained from NSGA-II algorithm were further analyzed to enhance understanding of respective behavioral characteristics. In this context, Pareto front of multi-objective optimization problem comprised a set of non-dominated solutions. Each represented distinct trade-offs between minimizing probability of piping system failure and reducing total inspection costs, which included both direct and indirect expenses.

Figure 5 shows the convergence of NSGA-II algorithm for the case study across 250 generations. The convergence of the algorithm was developed by a normalized hypervolume indicator (Beume et al., 2007; Kuo et al., 2023. In addition, the algorithm converged after 62 generations, showing its ability to minimize probability of failure and the total inspection cost across diverse probabilities, namely mutation rates.

The objective function values derived from both the initial and efficient solutions are shown in Table 10. The efficient solution was determined using utopia method, as shown in Figure 6. Based on the results, the efficient solution was also analyzed using the same inspection cost. This was achieved by combining inspection methods during the final period with different related effectiveness, thereby significantly reducing probability of failure.

Table 10. The comparison of the solutions results derived from addressing the case study.

	Initial solution	**Efficient solution**
Total inspection cost (first objective function)	50,800	50,800
Total probability of failure (second objective function)	$1.631\ 10^{-1}$	$0.8975\ 10^{-1}$

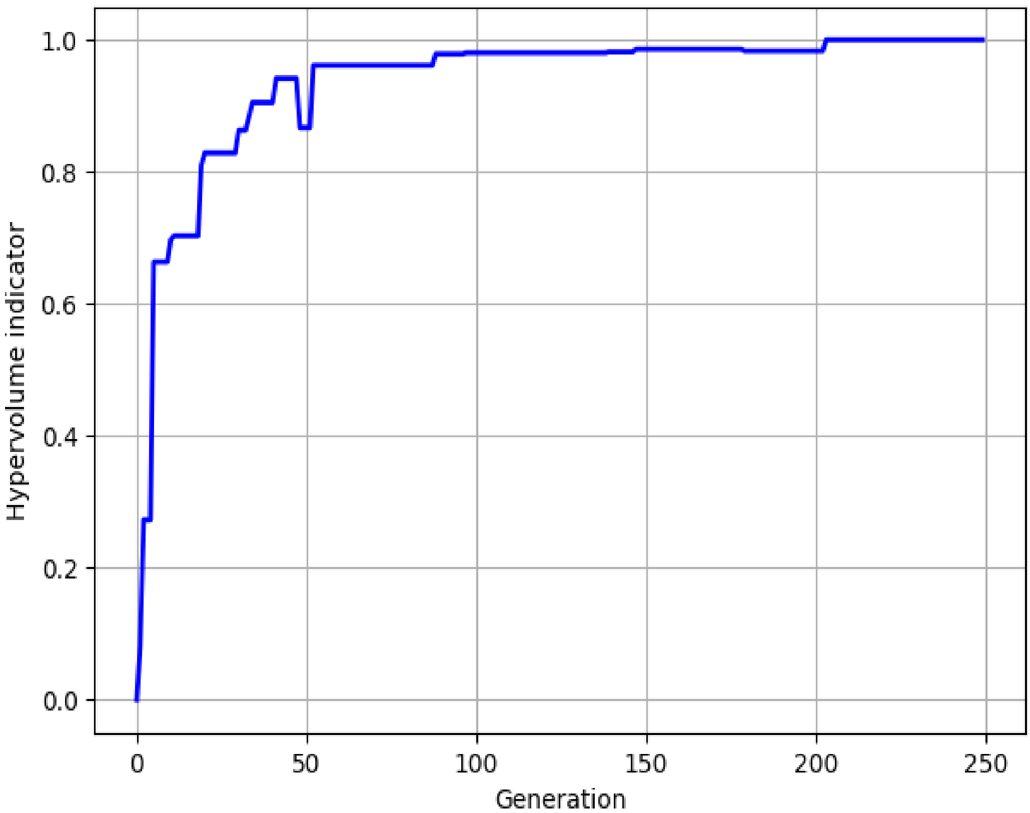

Figure 5. Convergence of NSGA-II algorithm for the case study.

The service life of piping systems can be extended by improving the accuracy of corrosion rate estimation using data collected across multiple inspection periods. The method helped reduce the uncertainty associated with corrosion rate predictions, making it more reliable and predictable over time. Considering that the corrosion rate is the main source of uncertainty in integrity assessments, improving its accuracy is critical to extending asset life. In addition, more precise and reliable inspection methods are required to effectively detect equipment flaws, particularly in piping systems, where early identification of defects is essential for maintaining structural integrity and ensuring safe operation.

This present study has practical implications for asset integrity management. This was observed by enabling the integration of NSGA-II-generated dynamic inspection schedules into existing maintenance systems, such as CMMS and RBI platforms. Optimized inspection intervals and priorities can be directly translated into work orders and inspection plans. Meanwhile, multi-objective outputs (risk–cost trade-offs) supported informed decision-making under operational constraints. The framework also served as a decision-support module, which continuously refined the schedule. The updated inspection data received, further enabled adaptive, risk-informed maintenance planning.

The results of this study may have inherent limitations that require further investigation. Although the effectiveness of each NDE method has been evaluated, uncertainties arising from data inaccuracies in corrosion rate estimation, particularly in relation to inspection tools and operator performance, have not been explicitly integrated into the model. Another limitation centered on the estimation of probability of failure, which was strongly governed by the corrosion rate. Furthermore, this was determined using a deterministic method. The model could be further improved by adopting a less conservative and more realistic method to estimating corrosion rates. For example, the integration of multiple inputs to identify potential corrosion mechanisms, including fluid characteristics (Effendi et al., 2020; Noegroho Hadi 2023; Permana et al., 2025).

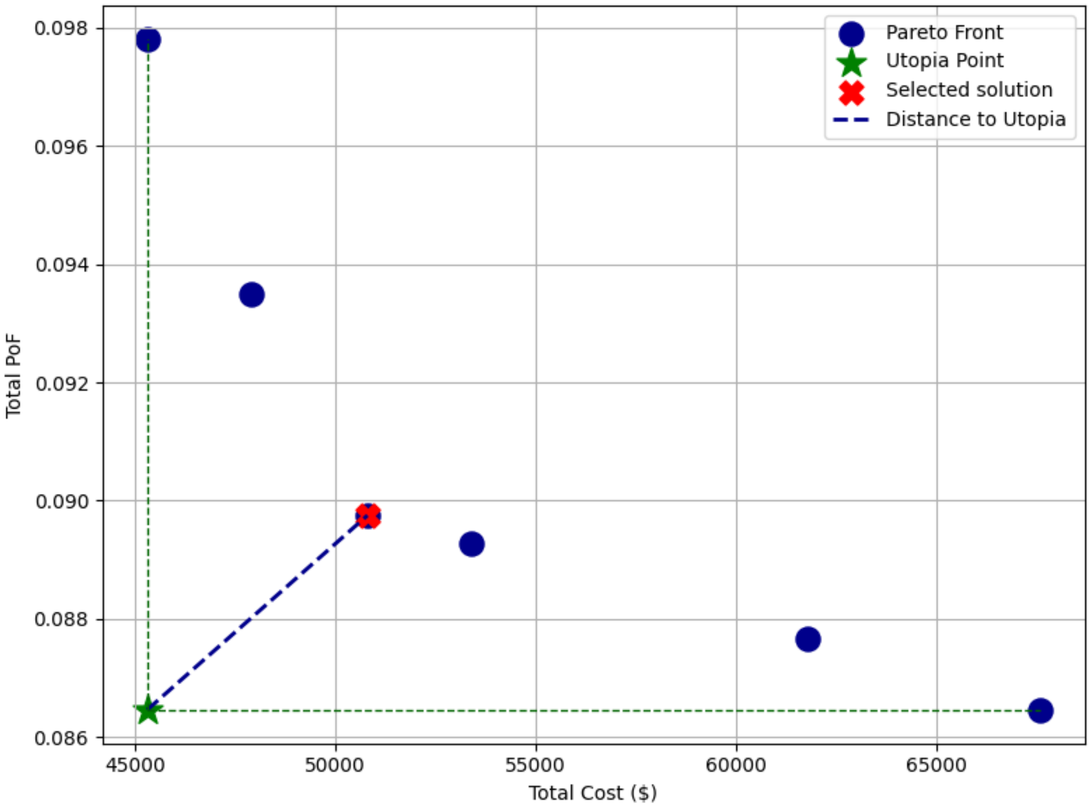

Figure 6. Selection of the optimal solution from Pareto front using utopia point method.

CONCLUSION

In conclusion, this study focused on inspection methods of piping systems that balanced risk reduction and cost optimization. The method enabled effective inspection that accounted for acceptable risk thresholds and budget constraints. It examined different methods used to identify the safest and most cost -effective options. Optimized solution reduced the total probability of failure from 1.631 10^{-1} to 0.8975 10^{-1} while maintaining the same total inspection cost of 50,800, showing a substantial improvement in reliability without additional economic burden.

The results showed that reasonable spending produced an extremely low risk profile and avoided unnecessary costs. The framework allowed for customized inspection plans across real-world applications. Moreover, probability of failure and overall costs served as optimization objectives, which relieved users of the need to determine the maximum acceptable risk or perform complex calculations.

This study also included ingenious mutations to improve algorithm performance and find faster solutions. The method has been proven to solve practical challenges in oil and gas sector, showing its effectiveness. Further studies need to incorporate additional optimization algorithms such as NSGA-III and MOPSO. Uncertainties arising from data inaccuracies must also be systematically incorporated to improve the robustness and reliability of the model. The proposed model could be enhanced by integrating artificial intelligence to handle complex data, thereby achieving faster and better performance, considering that the objective function is data driven.

DECLARATIONS

Author contribution

Tri Wahono: Writing - original draft, Conceptualization, Methodology, Visualization. Imam Mukhlash: Writing - review & editing, Methodology, Supervision. Endah R.M. Putri: Writing - Review & Editing, Methodology, Supervision. Agung Purniawan: Writing - Review & Editing, Methodology, Supervision.

Funding statement

None.

Competing interest

The authors declare no known competing financial interests or personal relationships that could have influenced the work reported in this study.

The use of AI or AI-assisted technologies

None.

GLOSSARY OF TERMS AND SYMBOLS

Term & Symbol	Definition	Unit
AHP	Analytical Hierarchy Process	
API	American Petroleum Institute	
C_{allow}	Corrosion Allowance	mmpy
CMMS	Computerized Maintenance Management Systems	
CoF	Consequence of Failure	
D_f	Damage Factor	
FC	Financial Consequence	
FMS	Management System Factor	
gff	Generic Failure Frequency	
GWT	Guided Wave Testing	
HT	Hydrostatic Testing	
MOGA	Multi-objective Genetic Algorithm	
NSGA-II	Non-dominated sorting genetic algorithm-II	
PoF	Probability of Failure	
t_{min}	Minimum required wall thickness	mm
TOPSIS	Technique for Order of	

	Preference by Similarity to Ideal Solution	
t_{rd}	Thickness reading	mm
UTM	Ultrasonic Thickness Measurement	

REFERENCES

Abubakirov, R., Yang, M., et al., (2020), A risk-based approach to determination of optimal inspection intervals for buried oil pipelines. Process Safety and Environmental Protection, 134, 95–107. https://doi.org/10.1016/j.psep.2019.11.031

Aditiyawarman, T., Kaban, A. P. S., et al., (2023), A Recent Review of Risk-Based Inspection Development to Support Service Excellence in the Oil and Gas Industry: An Artificial Intelligence Perspective. ASCE-ASME Journal of Risk and Uncertainty in Engineering Systems, Part B: Mechanical Engineering, 9(1). https://doi.org/10.1115/1.4054558

API RP 580. (2023). Elements of a Risk-Based Inspection Program. In API (Fourth Ed., Issue August). American Petroleum Institute.

API RP 581, (2025), Risk-Based Inspection Technology. January.

Asyik, N., Latief, R. U., et al., (2026), Testing Center for Oil and Gas Risk - Informed Strategic Governance in Precast Concrete Production as A High - Risk Industry : Cross - Sector Evidence from The Construction and Oil & Gas Industries. *Scientific Contributions Oil and Gas*, 49(1), 459–474. https://doi.org/10.29017/scog.v49i1.1956

Beume, N., Naujoks, B., et al., (2007), SMS-EMOA: Multi-objective selection based on dominated hypervolume. European Journal of Operational Research, 181(3), 1653–1669. https://doi.org/10.1016/j.ejor.2006.08.008

Campari, A., Vianello, C., et al., (2024), Machine learning-aided risk-based inspection strategy for hydrogen technologies. Process Safety and Environmental Protection, 191(PA), 1239–1253. https://doi.org/10.1016/j.psep.2024.09.031

Deb, K., Pratap, A., et al., (2002), A fast and elitist multi-objective genetic algorithm: NSGA-II. IEEE Transactions on Evolutionary Computation, 6(2), 182–197. https://doi.org/10.1109/4235.996017

Effendi, D., Hani, B., et al., (2020), Determination of Water Characteristics at Gathering Station oil Field Y According to Minister of Environment Regulation No . 19 Year 2010. *Lembaran Publikasi Minyak Dan Gas Bumi*, 54(2), 111–125.

Huang, W. L. Z. Z. S., (2020), Knee Point-Guided Multi-objective Optimization Algorithm for Microgrid Dynamic Energy Management.pdf. Wiley.

Javid, Y., (2021), A bi-objective mathematical model to determine risk-based inspection programs. Process Safety and Environmental Protectionpro, 11(1), 893–904. https://doi.org/10.1016/j.psep.2020.12.022

Javid, Y., (2025), Efficient risk-based inspection framework: Balancing safety and budgetary constraints. Reliability Engineering and System Safety, 253(January 2024), 110519. https://doi.org/10.1016/j.ress.2024.110519

Kuo, R. J., Edbert, E., et al., (2023), Applying NSGA-II to vehicle routing problem with drones considering makespan and carbon emission. Expert Systems with Applications, 221(February), 119777. https://doi.org/10.1016/j.eswa.2023.119777

Moura, M. D. C., Lins, I. D., et al., (2015), A multi-objective genetic algorithm for determining efficient risk-based inspection programs. Reliability Engineering and System Safety, 133, 253–265. https://doi.org/10.1016/j.ress.2014.09.018

Niu, Y. Y., & Li, X. J., (2025), A dynamic utopia point updating strategy for multi-objective optimization. ISA Transactions, 162(April), 37–46. https://doi.org/10.1016/j.isatra.2025.04.030

Noegroho Hadi., (2023), Pengawasan Korosi Di Unit Pengolahan Minyak Mentah. *Lembaran Publikasi Minyak Dan Gas Bumi*, 18.

Omar, A., & Moselhi, O. (2026). Multi-objective optimization model for automated risk-based inspection planning for concrete bridges. Automation in Construction, 181(PA), 106608. https://doi.org/10.1016/j.autcon.2025.106608

Permana, M. S., Soeweify, M. P., et al., (2025), Innovation in Inspection Planning Using the Corrosion Assessment Information System (CAIS) Analytical Tool to Prevent Stationary Equipment Failure in Crude Distillation Unit (CDU). *Scientific Contributions Oil and Gas*, 48 (3), 203–214. https://doi.org/10.29017/scog.v48i3.1848

Rachman, A., & Ratnayake, R. M. C., (2019), Machine learning approach for risk-based inspection screening assessment. Reliability Engineering & System Safety, 185, 518–532. https://doi.org/https://doi.org/10.1016/j.ress.2019.02.008

Seo, J. K., Cui, Y., et al., (2015), A risk-based inspection planning method for corroded subsea pipelines. Ocean Engineering, 109, 539–552. https://doi.org/10.1016/j.oceaneng.2015.07.066

Sözen, L., Yurdakul, M., et al., (2022), Risk-based inspection planning for internal surface defected oil pipelines exposed to fatigue. International Journal of Pressure Vessels and Piping, 200(August). https://doi.org/10.1016/j.ijpvp.2022.104804

Szparaga, A., Stachnik, M., et al., (2019), Multi-objective optimization based on the utopian point method applied to a case study of osmotic dehydration of plums and its storage. Journal of Food Engineering, 245 (December 2017), 104–111. https://doi.org/10.1016/j.jfoodeng.2018.10.014

Tang, J., Wang, H., et al., (2023), Surrogate-assisted multi-objective optimization via knee-oriented Pareto front estimation. Swarm and Evolutionary Computation, 77(September 2022), 101252. https://doi.org/10.1016/j.swevo.2023.101252

Teurupun, A., Nugroho, B. S., et al., (2024), Risk-Based Inspection Analysis of Api 581 Pressure Safety Valve and Stripper Acid Gas Removal Unit at PT. XY. *Scientific Contributions Oil and Gas*, 47(3), 313–325. https://doi.org/10.29017/SCOG.47.3.1645

Wahono, T., Purniawan, A., et al., (2025), Risk-based asset integrity management in the oil and gas industry from traditional to machine learning approaches: A systematic review. Results in Engineering, 28(September), 107287. https://doi.org/10.1016/j.rineng.2025.107287

Weber, M., (2006), Some Safety Aspects on the Design of Sparger Systems for the. Process Safety Progress, 25(4), 326–330. https://doi.org/10.1002/prs

Zhang, K., Shen, C., et al., (2021), Knee based multimodal multi-objective evolutionary algorithm for decision making. Information Sciences, 544, 39–55. https://doi.org/10.1016/j.ins.2020.07.057